Critical Analysis of Network Defects in Cross-Linked Isobutylene-Based Elastomers by NMR Imaging

ARTICLE *in* MACROMOLECULES · JUNE 1999

Impact Factor: 5.8 · DOI: 10.1021/ma9902448

Critical Analysis of Network Defects in Cross-Linked Isobutylene-Based Elastomers by NMR Imaging

Peter Adriaensens, Anne Pollaris, Dirk Vanderzande, and Jan Gelan*

Department SBG, Instituut voor Materiaalonderzoek (IMO), Limburg University, Universitaire Campus, B-3590 Diepenbeek, Belgium

Jeffery L. White,*,‡ Anthony J. Dias, and Mauritz Kelchtermans†

Exxon Chemical, Polymer Science and Butyl Technology Divisions, 4500 Bayway Drive, Baytown, Texas 77520-9728

Received February 19, 1999; Revised Manuscript Received May 18, 1999

ABSTRACT: The analysis of chemical and physical network heterogeneities has been carried out for synthetic isobutylene-based elastomers using ^{1}H spin echo NMR imaging. Spatial homogeneity was compared for isobutylene−*p*-methylstyrene−*p*-bromomethylstyrene (PIB−PMS/BrPMS) terpolymers cured with inorganic versus organic curatives and unfilled materials versus those filled with carbon black. Surprising differences in the network structure were found for materials cured with an inorganic curative (ZnO) relative to those cured with an organic curative (1,6-hexamethylenediamine). Voids and void distributions were found to be an important performance variable on the basis of comparisons between the NMR imaging data and mechanical testing. Systematic comparison of solvent images and polymer images revealed the optimum experimental conditions for enhancing network density contrast or detecting microvoids. For the first time, direct ^{1}H images of polymer spins in a fully compounded, commercial polyisobutylene-based elastomer were acquired in the absence of any swelling solvent. Multislice imaging experiments were investigated as a method to construct three-dimensional void densities in elastomer compounds. Chemical-shift selective polymer imaging was used to selectively obtain network density information for either component of a two-phase blend containing the PIB−PMS/BrPMS terpolymer and polybutadiene. The ability of NMR imaging to provide data over statistically relevant sampling areas (hundreds of mm^3) for both neat polymers and fully compounded commercial materials (containing carbon black) represents a unique advantage over microscopic imaging methods for material property analyses.

Introduction

Our goal is to interrogate the chemical and physical details of isobutylene-based elastomer networks and to use the data to guide the selection of cure chemistries, compound formulations, and processing conditions. To this end, we have found the bulk length scale information provided by NMR imaging to be extremely informative with regard to both network homogeneity and defect distributions. The adaptation and application of NMR imaging methods to solid materials have understandably been most rapid in the area of elastomers, given their high molecular mobility (and therefore long T_2) at moderate temperatures.[1−3] A thorough review on the subject of NMR imaging of elastomers has recently been published by Blumich et al.[4] Previous reports on NMR imaging of elastomers have focused on cross-linking and aging in butadiene,[5−7] styrene-butadiene,[8] or natural rubber.[9,10] The analysis of solvent diffusion into polybutadiene has also recently been reported.[11]

Our interest in isobutylene-based elastomers stems from the unique characteristics of this polymer, in that even though the T_g is comparable to polybutadiene or polyisoprene, the chain dynamics are significantly reduced due to the steric constraints associated with methyl group packing.[12,13] Spin diffusion is efficient, leading to short T_2 relaxation times for polyisobutylene at room temperature.[14] Detailed NMR imaging data for polyisobutylene-based elastomers is noticeably absent from the literature, most likely due to the unusually short T_2 relaxation times relative to other elastomers. Koenig et al. used solvent imaging to investigate swollen butyl rubber that was cross-linked but unfilled.[15] Isobutylene−*p*-methylstyrene−*p*-bromomethylstyrene (PIB−PMS/BrPMS) terpolymers offer promise as a second-generation butyl rubber, since the gas-barrier properties of regular butyl rubber (isobutylene-*co*-isoprene) are maintained, while the resistance to oxidative degradation is enhanced by the saturated polymer backbone.[16]

We have used spin-density, T_2-weighted, T_1-weighted, and chemical shift selective NMR imaging methods to investigate elastomers swollen with either an aprotic, aromatic, or aliphatic solvent. Systematic comparisons of the polymer images and solvent images have defined the optimum experimental conditions for enhancing contrast of network density or for detection of voids. We find significant differences in the cross-link homogeneity for elastomers cured with an inorganic curative (ZnO) compared to those cured with a organic curative (1,6-hexamethylenediamine). Chemical shift selective images have been used to selectively probe cure states and defects in either component of blends made from the PIB−PMS/BrPMS terpolymer and polybutadiene. We report, for the first time, direct polymer images from an unswollen polyisobutylene sample.

Experimental Section

All MRI images were obtained on a Varian Inova 400 spectrometer (9.4 T), equipped with an imaging probe having an inner diameter of 25 mm. Data were obtained at room

* To whom correspondence should be addressed.
† Exxon Chemical Europe, Hermeslaan 2, B-1831 Machelen, Belgium.
‡ E-mail: Jeff.L.White@exxon.com.

10.1021/ma9902448 CCC: $18.00
Published on Web 06/16/1999

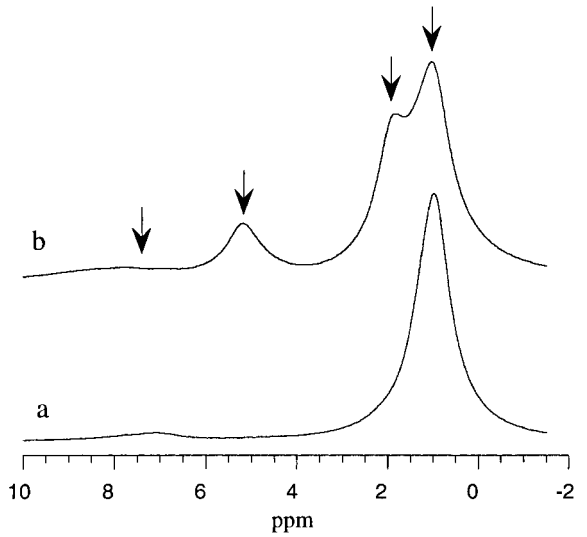

Figure 1. ^{1}H spectrum of (a) a PIB−PMS/BrPMS terpolymer and (b) a PIB−PMS/BrPMS blend with polybutadiene, both swollen in CCl_4, acquired with the imaging probe.

temperature unless otherwise noted. Images were acquired in a field of view of 25 × 25 mm with an in-plane resolution of 100 × 100 μm. Slice thicknesses are 1 mm, unless otherwise noted, corresponding to a gradient strength of 17−18 G/cm in the *z* direction. Typical gradient strengths were 2.5−6 G/cm for both the read and phase-encoding directions.

Images of samples swollen in CCl_4 and C_6H_{12} were obtained with a classical spin-warp pulse sequence in which slice selective 90° and 180° sinc pulses were used.[17] Images of samples swollen in C_6H_6 were obtained using a chemical shift selective but nonslice selective 90° Gaussian pulse of 5 ms, followed by a slice selective 180° sinc pulse (800 μs). All images were acquired using 12 accumulations.

Images of the polymer spins in a swollen sample were obtained with a repetition time TR = 1 s and an echo time TE = 11−13 ms (slightly T_2-weighted spin density image) or TE = 25 ms (T_2-weighted images). For images of the solvent only, TR = 3 s and TE = 11−13 ms were used. Since solvents in general have a longer T_{1H} than the polymer, a longer repetition time is required.

Calculated spin density (M_0) and T_2 images were obtained out of a series of 20 chemical shift selective polymer images (swollen in C_6H_6), acquired as a function of the echo time TE (TE varried from 11 to 125 ms; TR = 2 s). By fitting the intensity of each pixel to the equation $\ln(M) = \ln(M_0) - TE/T_2$, the T_2 and M_0 images are obtained out of the slope and ordinate, respectively. So, all protons having a $T_2 = 4-5$ ms (shortest TE is 11 ms) will be detected and appear in the M_0 and T_2 images. Spots containing no protons or protons with a $T_2 < 4-5$ ms will appear black in both the T_2 and M_0 image.

For the PIB−PMS/BrPMS blends with polybutadiene, samples were swollen in CCl_4. Non-chemical shift selective images show both the aliphatic and olefinic components. The repetition delay was increased to TR = 2.5 s because of the longer T_{1H} of the polybutadiene resonances. For reference, a typical ^{1}H spectrum of the swollen blend (CCl_4) is shown in Figure 1. Signals are observed for the PIB−PMS aliphatic hydrogens (ca. 1 ppm; T_{1H} ca. 0.2 s), aromatic PIB−PMS hydrogens (ca. 7.5 ppm), olefinic hydrogens from polybutadiene (ca. 5 ppm; T_{1H} ca. 1.1 s), and aliphatic polybutadiene signals (ca. 1.9 ppm; T_{1H} ca. 0.5 s). The chemical shift selective images showing either the olefinic or aliphatic component were measured using 64 accumulations and a TR = 1.5 or 2.5 s for respectively the aliphatic or olefinic image.

The results of the statistical void analysis are an average over 90 slices of 200 μm in thickness. Herefore, three cylindrical samples (cut after swelling) with a diameter of 15 mm were examined over 30 slices each.

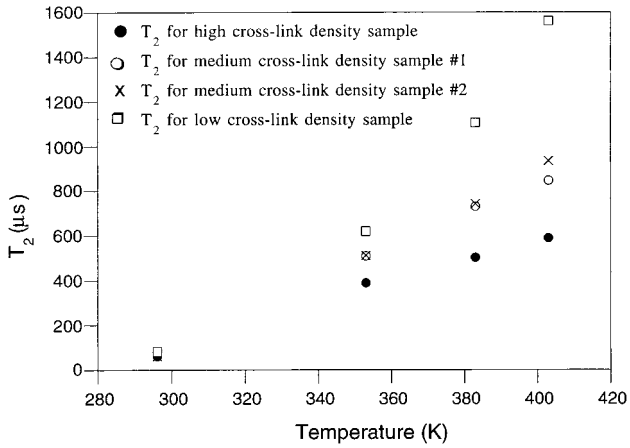

Figure 2. ^{1}H T_2 relaxation times vs temperature for four different cure states of PIB−PMS/BrPMS terpolymers.

Scheme 1

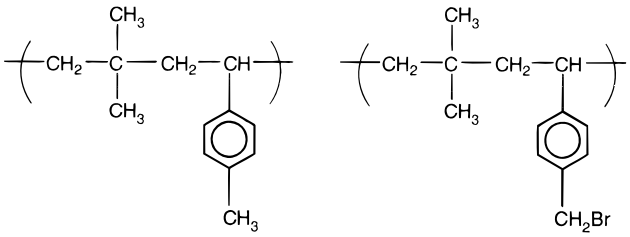

The direct polymer images of the dry, unswollen PIB−PMS/BrPMS terpolymer were obtained in a 16 mm coil using the standard spin-warp imaging sequence and at a temperature of 333 K.

Results and Discussion

The structure of the PIB−PMS/BrPMS terpolymer is shown below in Scheme 1. The terpolymer contains 97−98 mol % PIB, and as such the chain dynamics and relaxation properties are similar to neat polyisobutylene. Cross-linking in this terpolymer occurs through the BrPMS functionality.[16] Inorganic or bifunctional organic curatives may be used to cross-link this terpolymer.

The ^{1}H T_2 values are 60 μs at room temperature for PIB, which is nominally too short for direct imaging using standard methods. Plots of the ^{1}H T_2 relaxation times from static CPMG experiments are shown in Figure 2 for some of the cross-linked PIB−PMS/BrPMS terpolymers used in this study. One observes that at room temperature the relaxation properties are independent of cross-link density, since chain dynamics are controlled by the steric constraints of methyl packing. However, at elevated temperatures, one observes a significant dispersion in T_2 values due to differences in the overall cure state. In fact, the sensitivity of T_2 relaxation times obtained from static CPMG measurements to small changes in cross-link density is high at elevated temperatures. Shown in Figure 3 is a plot comparing the T_2 values measured at 120 °C to cross-link density data measured by a mechanical oscillating disk rheometer. The observed correlation is indeed linear and extrapolates to the experimentally determined value for an uncured sample. This was verified using a neat polyisobutylene sample which contained no cross-links; the T_2 was measured as 1720 μs. One could clearly exploit this relationship for process control in elastomer curing processes using currently available low field benchtop NMR instruments.[4]

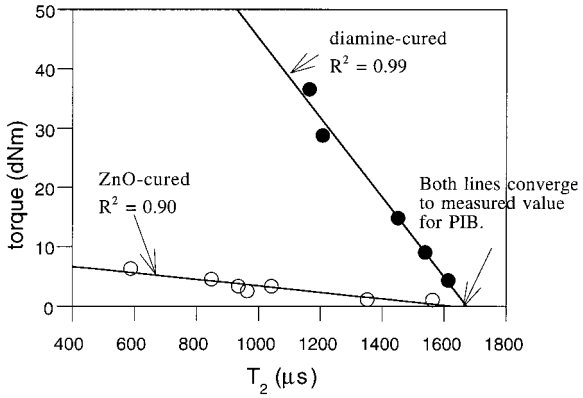

Figure 3. ^{1}H T_2 values (measured at 120 °C) vs rheometer data for ZnO-cured (○) and diamine-cured (●) PIB−PMS/BrPMS terpolymers.

Given that the ^{1}H T_2 is too short to directly image the isobutylene polymers at room temperature, swelling solvents were used to facilitate image acquisition using standard spin echo methods. Figure 4 shows images obtained using different solvents, and imaging either the solvent or the polymer, for an unfilled, "loosely" cross-linked sample of PIB−PMS/BrPMS (0.7 mol % BrPMS). The image in Figure 4a arises from both the cyclohexane solvent and the polymer, since the aliphatic signals from each overlap. The image is heterogeneous in terms of contrast (note the mottled appearance) and signal density (dark circles). Figure 4b was obtained using the aprotic solvent CCl_4. All signals in this image necessarily arise from the polymer itself, with no interference from the solvent. Again, one observes light and dark polymer regions, as well as the dark circular spots which contain no signal. The identification of these dark circular features will be discussed in the following section. Parts c and d of Figure 4 compare a benzene-swollen sample in which either the benzene or the polymer (respectively) was selectively imaged via a chemical shift selective pulse sequence (aromatic vs aliphatic signal excitation). The dark circular spots are more clearly resolved in the solvent image, whereas the contrasting polymer regions are more easily distinguished in the aliphatic chemical shift image of the polymer spins. Parts c and d of Figure 4 were obtained using TE = 13 ms. Enhancements in contrast for regions of different cross-link density may be realized by increasing the echo time, i.e., imposing a T_2 filter. The sample of part d is shown again in part e, but following acquistion with TE = 25 ms. The randomly distributed white circular regions correspond to more mobile areas in the network and are enhanced relative to the image in Figure 4d obtained with TE = 13 ms. This sample was cured using ZnO as the curative. Other polymer spin experiments in which the repetition time TR was varied resulted in uniform attenuation of all signals across the image, indicating that all the polymer spins had similar T_{1H} values.

Another example of T_2-weighted contrast enhancement in the polymer-selective chemical shift images is shown in Figure 5. Parts b and c show images for an

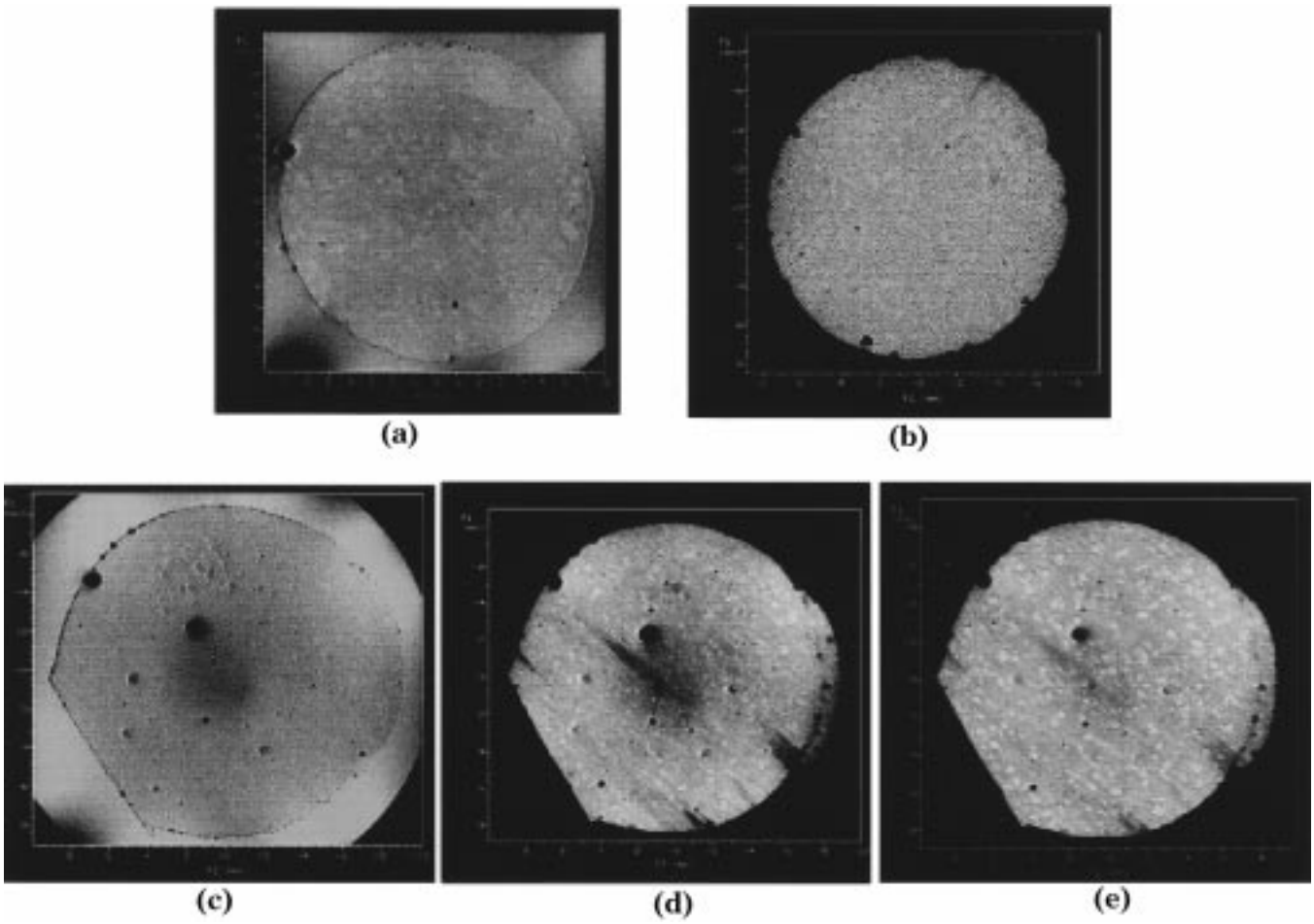

Figure 4. MRI images of an unfilled, ZnO-cured PIB−PMS/BrPMS terpolymer swollen in (a) cyclohexane, (b) CCl_4, and (c−e) benzene: (c) solvent image, (d) polymer image with TE = 13 ms, (e) polymer image with TE = 25 ms.

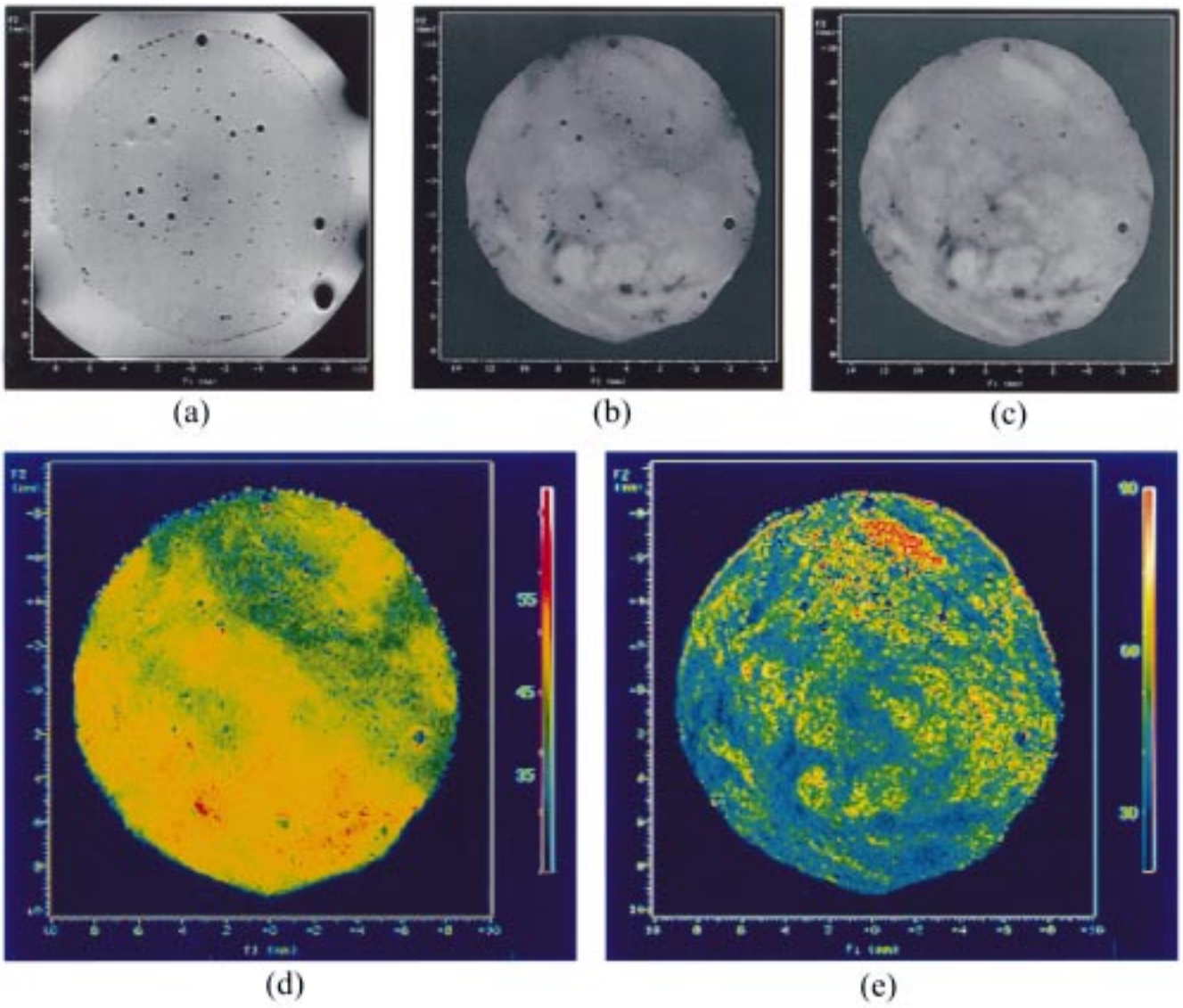

Figure 5. MRI images of an unfilled, diamine-cured PIB−PMS/BrPMS terpolymer swollen in benzene. (a) solvent image, (b) polymer image with TE = 13 ms, (c) polymer image with TE = 25 ms, (d) M_0 calculated polymer image, and (e) T_2 calculated polymer image.

unfilled PIB−PMS/BrPMS sample swollen in benzene, obtained using TE = 13 and 25 ms, respectively. The solvent image of the same slice location (a) shows the dark circular spots most clearly. A complex pattern of spatial deviations in cure states is enhanced in the image of Figure 5c. An organic curative, 1,6-hexamethylenediamine, was used to cross-link this sample. In addition to confirming that polymer selective imaging using long echo times is the best experimental strategy for detecting deviations in cross-link densities, comparison of the data in Figure 5b,c to that previously reported in Figure 4e shows that surpisingly different "patterns" of heterogeneity are observed depending on curative type.

Direct comparisons of calculated spin-density (M_0) and T_2 images for the 1,6-hexamethylenediamine cured sample in Figure 5a−c are shown in Figure 5d,e. Further, Figure 6 shows calculated spin density (M_0) and T_2 images for the ZnO-cured sample shown previously in Figure 4d,e, but at a different slice location. The T_2 images show T_2 values for benzene-saturated PIB rubber between 30 ms (very low-intensity regions) and 80 ms (high-intensity regions). Comparisons of the spin density images to the T_2 images for either sample reveals that the spatially distinct features in the image are inverted with respect to their intensity. This contrast inversion is consistent with our assignment of network heterogeneities (i.e., deviations in bulk cross-link densities) giving rise to intensity variations. The spin density image will be more intense in regions that are more tightly cross-linked, since there are more protons per unit area. Conversely, the intensity in the same area of the T_2-weighted image will be reduced, since the tightly cross-linked regions are less mobile, and therefore the decay of transverse magnetization is faster. Weakly cured regions appear light in the T_2 image. Comparison of parts d and e of Figure 5 shows these traits; both images show a fairly large "stripe" of weakly cross-linked elastomer in the upper center to middle right regions of the image. In general, T_2 dominates the M_0 effect. Poorly cured regions appear highly intense in the images although the spin density is somewhat lower (Figures 4d,e and 5b,c). The same "intensity inversion" characteristics are also observed in Figure 6a,b for the ZnO-cured sample. Again, light and dark regions are observed corresponding to differ-

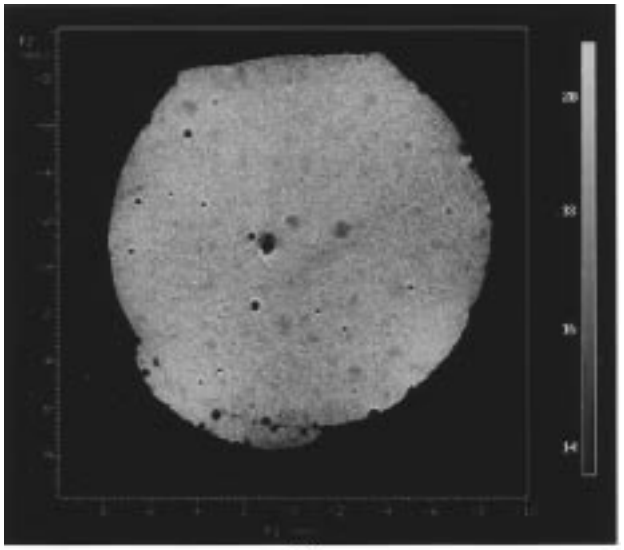

(a)

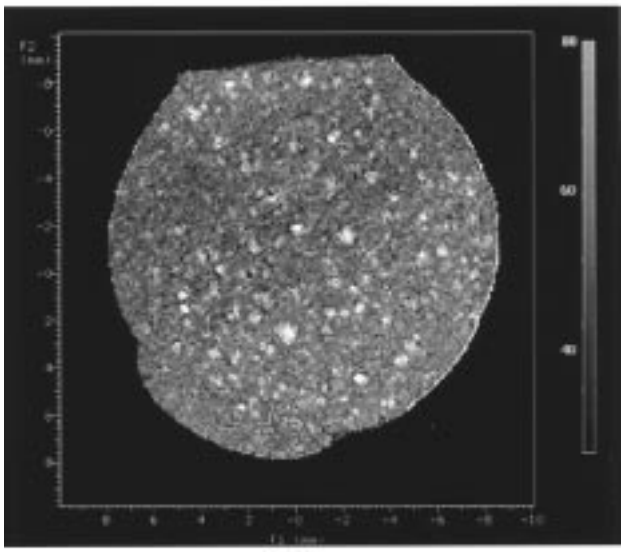

(b)

Figure 6. (a) M_0 calculated polymer image and (b) T_2 calculated polymer image of the unfilled ZnO-cured PIB−PMS/BrPMS terpolymer shown in Figure 4d,e, but at a different slice location.

ences in cross-link density. However, the topology of the heterogeneities observed in the ZnO-cured sample of Figure 6a,b is much different than that observed for the diamine-cured sample in Figure 5d,e. The ZnO samples have well-defined, circular regions of loosely cured polymer, while the diamine-cured samples exhibit irregular, swirled density gradients. These differences are consistent with what one would expect for dispersing a solid vs a liquid into a viscous medium. This result emphasizes the need to optimize mixing procedures for adequate dispersion of the curative in the polymer matrix based on the nature of the curative; obviously an inorganic solid like ZnO will require a different mixing strategy than an organic curative that is near or above its melting point.

We now present data which demonstrate that the dark, circular spots of negligible signal intensity observed in the previous images are voids in the elastomer. First, these black spots cannot be attributed to filler since they also appear in an unfilled rubber specimen

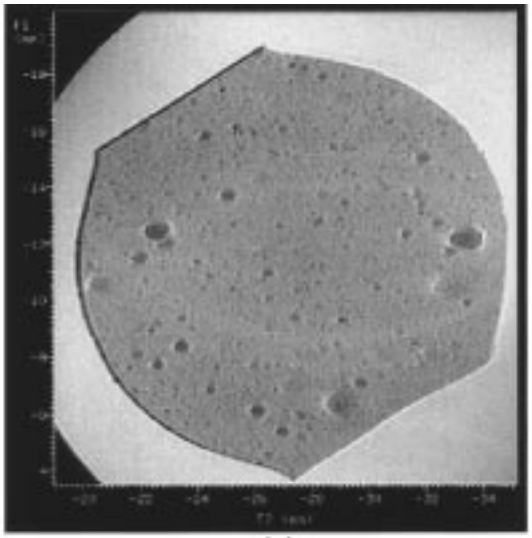

(a)

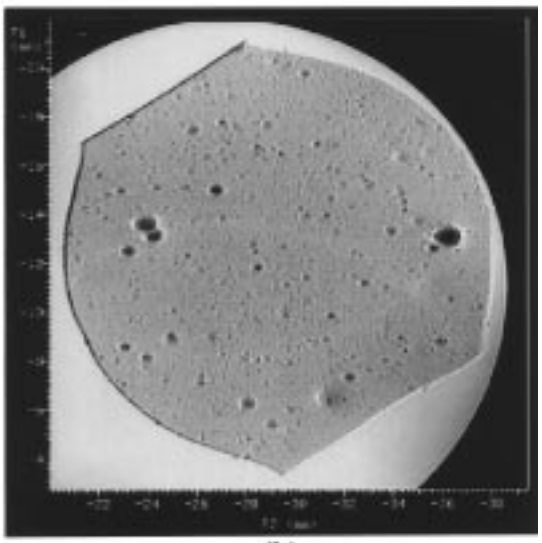

(b)

Figure 7. Solvent MRI images of a cured, carbon black-filled PIB−PMS/BrPMS terpolymer swollen in (a) benzene and (b) cyclohexane.

(Figures 4 and 5). Shown in Figure 7a is a solvent image for a cured, carbon black-filled, PIB−PMS/BrPMS sample swollen in benzene. This particular sample exhibits a large number of the dark circular spots, the larger of which are partially surrounded by bright intensity rings. The appearance of such bright fringes is expected if the dark spots are voids in the polymer, since severe magnetic susceptibility gradients exist at an air/polymer interface.[1] A similar experiment in which samples were swollen in cyclohexane gives identical features, again consistent with the presence of voids since no signal is observed for either the polymer or the aliphatic solvent. Surface tension prevents the solvent from entering the void. A particularly convincing confirmation for the void assignment is shown in Figure 7b. This image was obtained after the sample in Figure 7a was removed from benzene solvent, dried, reswollen in benzene, dried, and finally reswollen in cyclohexane. The cyclohexane solvent image in part b shows the same voids in the same position, and of the same dimension, as the original benzene image in part a. This confirms that the voids are inherent in the polymer and do not arise as an artifact from the swelling process. Also, the regular

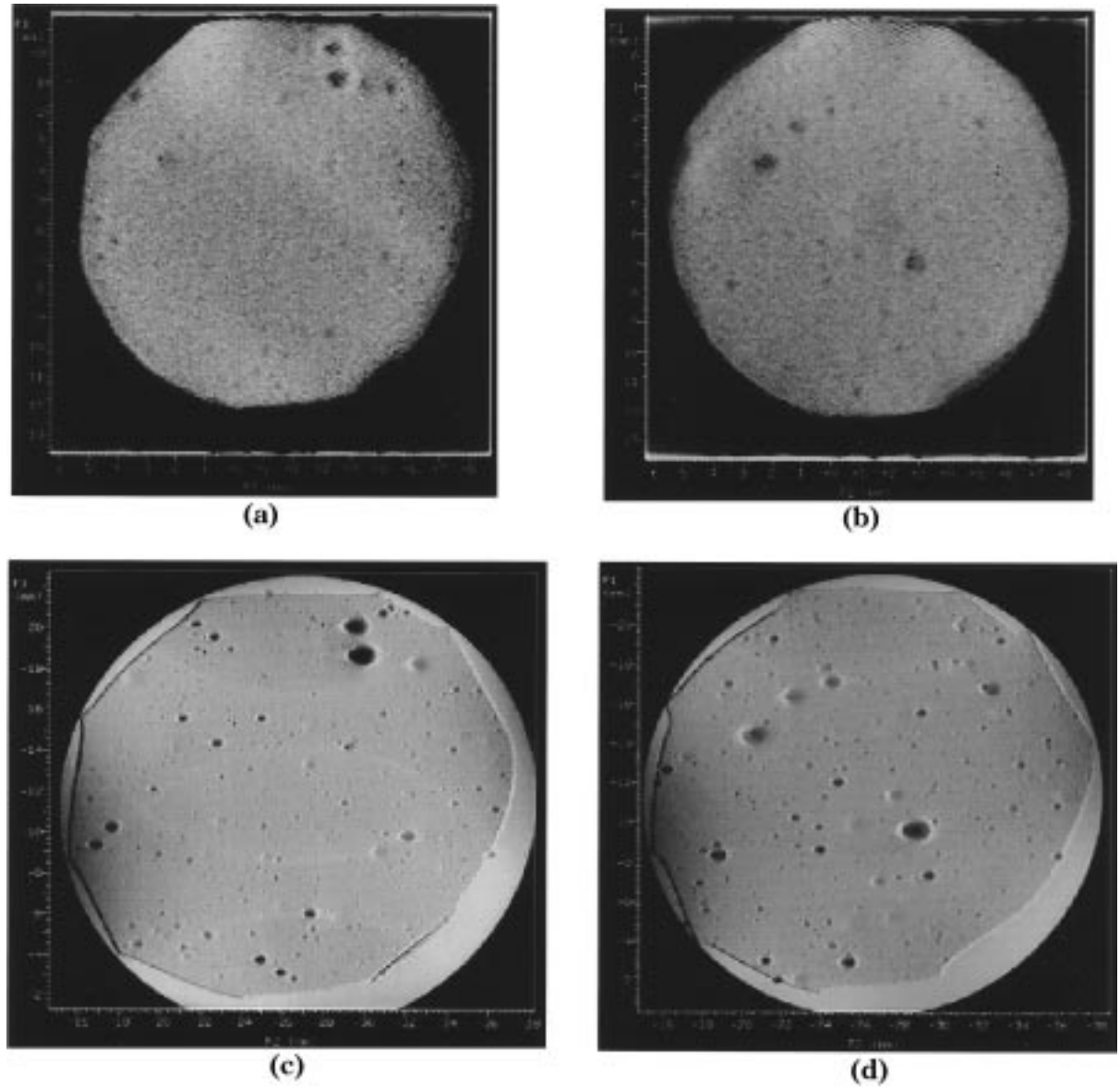

Figure 8. Images of two slice locations of (a, b) an unswollen (dry) cured and carbon black-filled terpolymer and (c, d) the same sample after swelling in cyclohexane.

shape and size of the dark spots discounts the possibility that they arise from highly cross-linked regions or paramagnetic or ferromagnetic centers (e.g., Zn agglomerates or iron particles). Moreover, the amount of curative is too small to account for the area occupied by these spots. Recalling the image in Figure 5d, one notes that there is no signal at all for the dark spots assigned as voids in the spin density image. We also note at this time that Kresja and Koenig have previously reported voids in swollen butyl rubber samples.[15] 3D reconstruction of a series of images, taken with a slice thickness of 150 μm, showed that the voids have a spherical shape.

A final and unambiguous result that confirms the identity of voids inherent in these compounded PIB−PMS/BrPMS elastomers is presented in Figure 8. Parts a and b show direct polymer images for two different slices obtained from an unswollen terpolymer sample (fully compounded with carbon black and cured) using a TE = 2 ms. Dark spots similar to what has already been assigned as voids are clearly present. The much shorter TE confirms this assignment. This image was obtained at 333 K. More importantly, images obtained for this same sample after swelling in C_6H_{12} (Figure 8c,d) show the presence of voids in the same positions. This demonstrates that, for elastomeric materials with T_2's short enough to prohibit straightforward acquisition of direct polymer images, representative data may be extracted from swollen materials.

The relevance of the void density data obtained in the NMR imaging experiment is demonstrated by the data in Figure 9. These samples are cured and filled (with carbon black) PIB−PMS/BrPMS compounds from commercial tests in which each sample was subjected to a combination of mechanical stress and heat cycles. Figure 9a shows three random slices from a compound which underwent >300 cycles before any failure occurred. The images from this sample show very few voids, and the few that are detected are small. The slices shown in Figure 9b are from a different compound that failed after only 1/10 of the number of stress/heat cycles survived by the compound in Figure 9a. Clearly, there exists a large number of voids, and several appear to

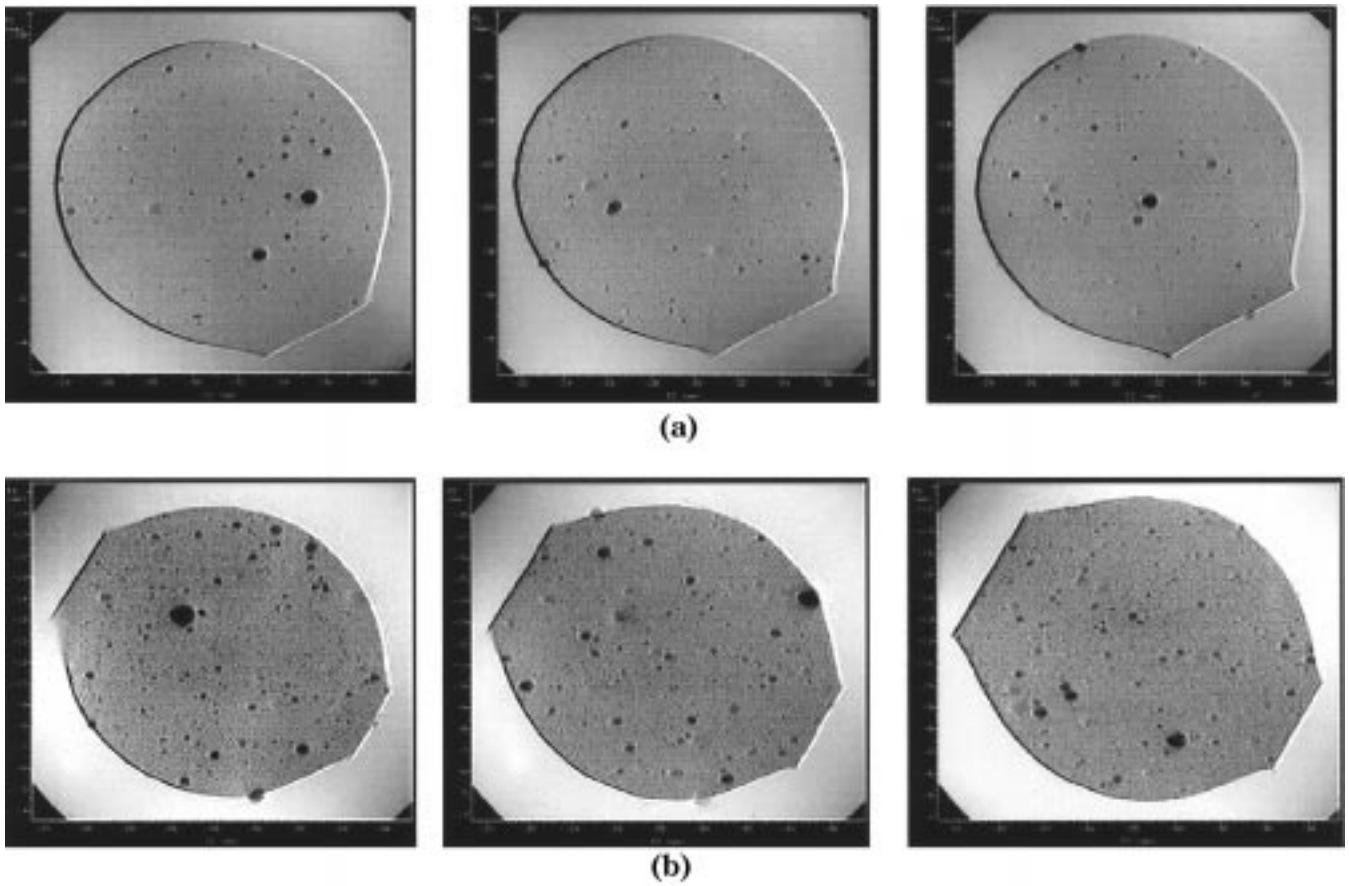

Figure 9. Solvent MRI images of cured and carbon black-filled PIB−PMS/BrPMS terpolymers, swollen in benzene. These polymers underwent a combination of mechanical stress and heat cycles: (a) >300 cycles before failure, (b) 1/10 of the number of cycles survived by the compound shown in (a).

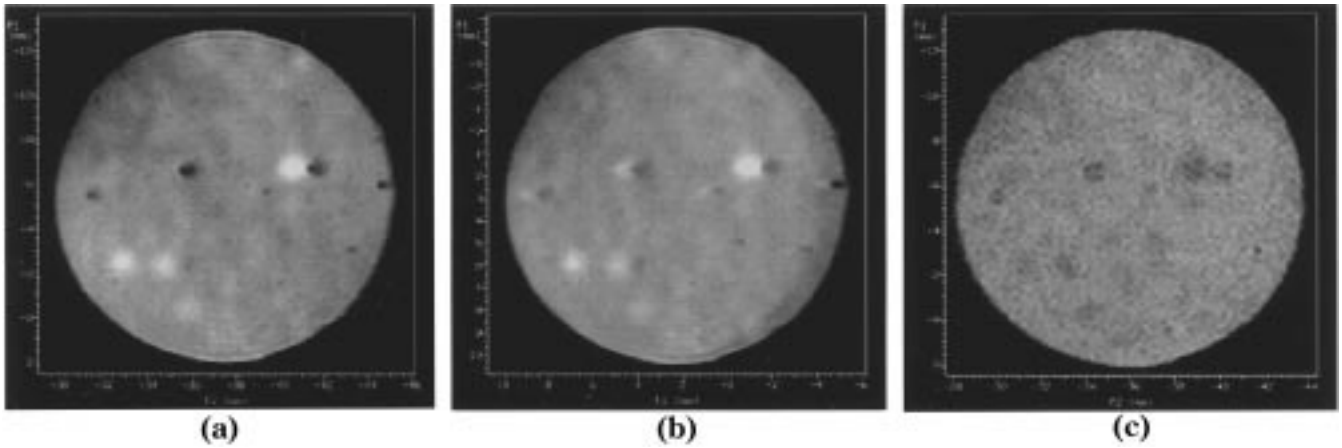

Figure 10. Chemical shift selective polymer images of a cured and carbon black-filled PIB−PMS/BrPMS blend with polybutadiene, swollen in CCl_4: (a) total ^1H image, (b) chemical shift selective image of the aliphatic components, (c) chemical shift selective image of the olefinic component.

be greater than 1 mm in diameter. Quantitative analysis of the void density in these samples shows that the material in part a (good performance) has an average of 72 voids per slice, while the poorly performing sample of part b has an average of 231 voids per slice. Several additional imaging experiments on a series of materials, in conjunction with the data here, indicate that void density critically controls the mechanical performance of commercial elastomer compounds. The presence of such a large number of imperfections will serve to concentrate stress/strain forces near the void, leading to premature failure of the compound. A detailed statistical analysis of this correlation between 3D NMR imaging-void density data (i.e., number of voids, average void area, next-nearest-neighbor distances, etc.) and mechanical performance is complete and will be reported in a separate contribution.

From these results we can conclude that solvent images are superior toward the visualization of void dimensions and density. Imaging of the polymer in swollen samples provides best visualization of heterogeneities in bulk cross-link densities. Although void

appearance does not depend on choice of swelling solvent, C_6H_6 can be advantageous in that either a solvent or polymer image may be obtained by chemical shift selection from the same slice location.

The data in Figure 9 demonstrated the utility of NMR imaging for analysis of commercial PIB−PMS/BrPMS compounds. Other applications involve its use as one component in a blend with polybutadiene and/or polyisoprene. A critical processing step in such an application involves the physical mixing of the polymeric blend components. Chemical shift selective imaging provides an avenue for selectively interrogating the nature and distribution of defects and mixing inhomogeneities in these blends by selectively imaging aliphatic hydrogens from the PIB−PMS component or olefinic hydrogens from the polybutadiene fraction. Shown in Figure 10a is the total ^{1}H image of a PIB−PMS/polybutadiene blend which is cured and filled with carbon black and compounded using a two-step mixing scheme. While one immediately notices the presence of voids, the overall resolution and contrast are necessarily poor due to multiple signal excitation. Shown in Figure 10b is the aliphatic selective image of both components in the blend. The resolution of voids is markedly improved, but a much more significant observation is the presence of several large, bright (white) regions in the slice. These same bright areas appear as dark regions in the olefinic selective image of the 5.0 ppm polybutadiene signal (Figure 10c). Given that these regions give a strong signal in the aliphatic image and a weak signal in the polybutadiene image, we conclude that these regions arise from undercured, highly mobile PIB−PMS/BrPMS chains. We rule out oil (present at a level of 9−11 wt %) as the cause of these bright areas in the aliphatic PIB−PMS/BrPMS image since no sharp peak is observed in the normal ^{1}H spectrum, and furthermore, the image is unchanged by swelling, drying, and reswelling. Presumably, this would lead to increased oil dispersion and a change in the image. The mixing scheme used to make this compound clearly does not result in a homogeneous distribution of the polymer components or curatives in the overall compound.

Conclusions

We have reported the details regarding the different types of network heterogeneities that are present in polyisobutylene-based elastomers and described experimental NMR imaging strategies to optimize detection of either cross-link density gradients or microvoids in the polymer. The spatial characteristics of the cross-linking gradients over areas of several millimeters was markedly different depending on what type of curative (ZnO vs 1,6-hexamethylenediamine) was used to cure the PIB−PMS/BrPMS terpolymer. Chemical shift selective imaging of the polymer spins was most sensitive to deviations in the network density, and selective interrogation of curing in either the PIB−PMS/BrPMS or polybutadiene component of blends was achieved using this approach. Selective imaging of the swelling solvent proved superior for detection of microvoid defects in both cured and cured/filled materials. For the first time, a direct ^{1}H image of the polyisobutylene elastomer was obtained and showed that indeed circular voids are present as defects in the material just as was detected using the solvent-based detection scheme. Statistical image analysis exercises showed that there was a direct correlation between the number of microvoids as measured by 3-D imaging and the mechanical performance (heat−stress cycles) of the elastomer compound. We propose that NMR imaging experiments such as those described here should be used in conjuction with traditional microscopy analysis (which suffers from small sampling areas) to provide a statistically relevant sampling of bulk structure, which may then be more accurately related to end-use performance.

References and Notes

(1) Chang, C.; Komoroski, R. A. *Macromolecules* **1989**, *22*, 600.
(2) Kuhn, W.; Barth, P.; Denner, P.; Muller, R. *Solid State NMR* **1996**, *6*, 295.
(3) Sarker, S. N.; Komoroski, R. A. *Macromolecules* **1992**, *25*, 1420.
(4) Blumler, P.; Blumich, B. *Rubber Chem. Technol.* **1997**, *70*, 468.
(5) Clough, R. S.; Koenig, J. L. *J. Polym. Sci., Polym. Lett.* **1989**, *27*, 451.
(6) Smith, S. R.; Koenig, J. L. *Macromolecules* **1991**, *24*, 3496.
(7) Rana, M. A.; Koenig, J. L. *Macromolecules* **1994**, *27*, 3727.
(8) Fulber, C.; Blumich, B.; Unseld, K.; Heermann, V. *Kautsch. Gummi. Kunstst.* **1995**, *48*, 254.
(9) Blumler, P.; Blumich, B. *Macromolecules* **1991**, *24*, 2183.
(10) Barth, P.; Hafner, S.; Denner, P. *Macromolecules* **1996**, *29*, 1655.
(11) Cody, G. D.; Botto, R. E. *Macromolecules* **1994**, *27*, 2607.
(12) Boyd, R. H.; Pant, P. V. K. *Macromolecules* **1991**, *24*, 6325.
(13) Boyd, R. H.; Pant, P. V. K. *Macromolecules* **1992**, *25*, 494.
(14) White, J. L.; Dias, A. J.; Ashbaugh, J. R. *Macromolecules* **1998**, *31*, 1880.
(15) Kresja, M. R.; Koenig, J. L. *Rubber Chem. Technol.* **1990**, *64*, 635.
(16) Merrill, N. A.; Powers, K. W.; Wang, H. C. *Polymer. Prepr.* **1992**, *33*, 962.
(17) Kumar, A.; Welti, D.; Ernst, R. R. *J. Magn. Reson.* **1975**, *18*, 69.

MA9902448